

Is there an influence of short-term solar activity variations on mesopause region airglow?

J. Scheer and E.R. Reisin

Instituto de Astronomía y Física del Espacio, UBA-CONICET, Ciudad Universitaria, 1428 Buenos Aires, Argentina
(jurgen@caerce.edu.ar / Phone: +54-11-4781-6755 ext 228)

Abstract

A-priori, rapid variations of solar activity that directly impact on the terrestrial environment should be expected to influence airglow brightness in the mesopause region via the photodissociative production of atomic oxygen, as it does on the time scale of the solar cycle. To find out whether this is supported by our midlatitude data, we analyze the strongest geoeffective solar activity events, in times when data from the Argentine airglow spectrometer were obtained. An alternative interaction path involving geomagnetic perturbations mediated by the solar wind can also be expected to affect the mesopause region. Daily mean values of different solar and geomagnetic activity indices, and more than 1400 nights of airglow brightness and rotational temperature measurements (mostly from El Leoncito, 31.8°S) are available for this study. The diagnostic value of this investigation is augmented by using information corresponding to two different nominal altitudes (87 km for the OH(6-2) band, and 95 km for the O₂b(0-1) band). Our approach ranks the (solar and airglow) events by their respective strength, which automatically provides emphasis on the more important cases. We conclude that if an airglow response to strong solar events exists, it is only short-lived and should therefore most easily be detectable by daytime observations. On the other hand, we did not find signatures in our airglow data that could convincingly be related to geomagnetic storms.

1. Introduction

Mesopause region airglow brightness and temperature are related to atomic oxygen and ozone concentration and therefore to the UV solar energy input at wavelengths of 140 to 200 nm responsible for their photochemical production. This applies similarly to the OH Meinel bands (from 87 km nominal altitude) as to the O₂ Atmospheric band (at 95 km). Therefore, a dependence of these parameters on solar activity could be expected, not only during the 11-year solar cycle, but possibly also at the time scale of individual solar flares (although here the response may be delayed, i.e. by the time needed for the downward transport of atomic oxygen into the airglow layers). However, we still cannot claim to have a good quantitative understanding of solar activity effects on the mesopause region, since even the energetically and chemically very important ozone mixing ratio at these altitudes has been successfully modelled only recently (Smith and Marsh, 2005).

At the time scale of the solar cycle, previous evidence about solar influence on mesopause airglow and temperature for different geographic locations has been so diverse as to comprise strong correlations as well as strong anticorrelations (see, for instance, Beig et al., 2003). We have previously not found a solar cycle effect, at the altitude of the OH emission (Scheer et al. 2005a). There was, however, quite a different behaviour in the O₂ emission, with transitions between strong correlation, anticorrelation, and uncorrelated variations, each lasting many months.

In addition to the photochemical excitation and heating due to solar flares, there may also be a mesopause region response to the geomagnetic storms that often follow coronal mass ejections associated with flare activity. As a recent example of geomagnetic activity affecting mesopause region airglow, there are the OI 558 nm observations during the very strong geomagnetic storm of 31 March 2001 by Balan et al. (2004), who report an emission increase of almost a factor of 2. If such a strong effect also exists in OH and O₂ airglow, it should be easily detectable in a single event.

Here, we attempt to determine if our airglow data obtained at lower midlatitudes contain evidence of short-term perturbations that can be attributed to impulsive solar activity events. Thereby, we exploit the availability of many uninterrupted blocks of night-to-night data in our data set that spans the interval from 1986 to 2006 (although fragmented by many long gaps).

2. Data sets and analysis philosophy

The airglow data used here are intensities and rotational temperatures of the OH(6-2) and O₂b(0-1) bands obtained with our airglow spectrometer (Scheer, 1987; see also Scheer and Reisin, 2001). They were acquired since June 1986 until June 2006, mostly from El Leoncito (31.8°S, 69.3°W), but in 1994 from Buenos Aires (34.6°S, 58.4°W), and in 1990 from El Arenosillo (Spain; 37.1°N, 6.7°W). Table 1 gives the number of nights of observations per month, in the years when data were available, showing the campaign-style data acquisition before 1997, and the less segmented measurements from 1998 to 2002/3 and in 2006. The good coverage of some of the years is important to increase the probability to monitor interesting solar events during several consecutive nights and eventually detect an airglow response within an appropriate time delay. On average, there is also good nocturnal coverage by more than 330 data for each parameter (corresponding to nearly 8 hours of data, discounting gaps). Unfortunately, missing data always increase the risk of losing important solar events. Thus, we missed cases like the strong geomagnetic storms of March 1989 and 2001, the X20 flare of 2 April 2001, and the Halloween events (Mannucci et al., 2005; Tsurutani et al. 2005) in October and November 2003.

For solar and geomagnetic activity data, we use the following information:

Lists of X-ray flare events (class M and X) measured by the GOES satellites were compiled from the YOHKOH SXT web site (<http://www.lmsal.com/SXT/homepage.html>), for August 1997 to February 2003, and February to June 2006.

Solar EUV data of the Solar Extreme Ultraviolet Monitor (SEM) on the SOHO satellite were downloaded from the University of Southern California web site (http://www.usc.edu/dept/space_science/sem_data/downloadSEM.html). Daily mean values from 1997 to June 2003, and 10-min averages for July and November 2000, April and December 2001 were used.

Daily observed solar radio flux (F10.7) from Ottawa/Penticton was accessed through the NGDC web site (ftp://ftp.ngdc.noaa.gov/STP/SOLAR_DATA/SOLAR_RADIO/FLUX/). These data are available since 1947, and here we used those until May 2006.

As a proxy for geomagnetic activity, the *Dst* index was obtained from the University of Kyoto web site (<http://swdcdb.kugi.kyoto-u.ac.jp/dst/dir>), for the years 1986 - 2003.

The general approach for the present analysis is as follows. Because of the limited information on solar activity available, none of which directly and completely points to an interaction with the mesopause region, it is necessary to investigate different solar radiation proxies (EUV, X-ray flare index, F10.7) and also geomagnetic activity (as *Dst* storm index) when comparing with airglow anomalies.

The information contained in these proxies is used to identify individual solar and geomagnetic activity events with respect to their timing and strength, for an objective survey. The X-ray flare index is already in the required form, but some processing is necessary to make the other proxies usable to specify solar events. For the *Dst* index, we localize the most negative deviation corresponding to a geomagnetic storm. In order to convert F10.7 flux into an indicator of solar events, it is necessary to remove the slow solar cycle variation. A simple way to do so is by subtracting from a daily value the average of several neighbouring values (we use ten). This high-pass filter is also applied to the EUV diurnal means to remove the baseline variation, which can be comparable to the amplitude of the flare.

The same filtering technique can also be used to characterize impulsive day-to-day airglow anomalies based on nocturnal means (as in Scheer et al., 2005b). Since there are many data gaps (nights without data), it is good to use a flexible approach that does not only work symmetrically but also allows for an

asymmetric or non-equal spacing of neighbouring nights. This avoids edge effects and other information loss.

The main difficulty in this whole analysis consists in discriminating solar effects from intrinsic atmospheric variability, which is not only very strong, but also unpredictable (see, e.g., [Scheer et al., 2005b](#)). By ranking all the observed events according to strength, our study focusses on the strongest events which are most likely to have detectable signatures, distinguishable from the intrinsic variability. During spells of low dynamical activity, weaker solar disturbances may be detectable, but also the opposite is true. We do not only try to answer the question “is there a mesopause region airglow response to a given solar event?”, but also the complementary one, “is there a solar/geomagnetic cause to an airglow event?”, to avoid drawing wrong conclusions about causal relationships based on only part of the available evidence.

3. Results and discussion

3.1. Is there a “best” proxy?

In order to look for a proxy most suitable for rapidly finding solar radiation events, we compared the ranking tables for the F10.7 and EUV “anomalies” (as explained above), together with the X-ray flare index. From data between August 1997 and December 2002, we find 144 dates where at least one of these proxies signals a solar event. Only 17% of the cases show up in two proxies, and none in all three. Clearly, no single proxy is capable of ranking all solar events. Among the cases that relate strong X-ray flares with a significant EUV signature, the four principal ones (also shown in Table 2) are those of 14 July 2000 (the class X5.7 flare known as the “Bastille Day” event), 26 November 2000 (class X4.0), 15 April 2001 (X14), and 28 December 2001 (X3.4). There are also strong F10.7 events that coincide with EUV or X-ray events. The strongest one occurs on 12 July 2000 accompanied by an X1.9 flare. However, none of the three pairs of parameters show any correlation with respect to event strength (i.e., one cannot predict the strength of a solar event in one proxy, from another proxy). This lack of correlation is no surprise. For example, there are known to be dramatic differences in spectral variability in a single flare by more than two orders of magnitude, for some UV line emissions, also with respect to radio emission close to 10 cm wavelength ([Brekke et al., 1996](#); mean differences over a wider spectral range may be much smaller). Another reason is, of course, the different temporal resolution of the data as used here. While F10.7 observations are only made at local noon, we use diurnal averages of EUV. In contrast, X-ray events are precisely timed.

Also, contamination by solar particles can become quite serious in the SOHO-SEM EUV data (see, e.g., [Meier et al., 2002](#), [Tsurutani et al., 2005](#)). This contamination varies between flares, and may be absent ([Tsurutani et al. 2005](#)). In our ranking, this effect exaggerates at least some of the EUV events, and may involve delays of the order of a day. As Fig. 1 for the Bastille event shows, the prompt EUV signature is followed by a steady rise of energetic particles that peaks only 26.5 hours after the EUV flare, surpassing the real EUV signal by a factor of 30. This shape probably mainly reflects the different arrival times due to the particle velocity spread. After arrival of the slowest particles, the signal dies down more rapidly. It is only because of the timing of the EUV flare that our daily averaged proxy locates the event on July 14 at all (and not only on the next day). This is certainly a particularly difficult case, and the other three cases mentioned above are much less disturbed by this contamination. However, these particle effects do not disqualify the SEM data as a proxy for impulsive solar activity events, because they may be geoeffective, in their own right. On the one hand, there are direct chemical changes in the middle atmosphere, including the mesopause region (e.g., [Jackman et al., 2004](#)). On the other hand, strong particle events can also trigger strong geomagnetic storms (via mechanisms reviewed in detail by [Gonzalez et al., 1999](#)).

3.2. Is there an airglow response to the Bastille flare?

The particles accompanying the Bastille Day event are indeed geoeffective, because strong geomagnetic activity starts 34 hours after the flare, as shown by the very strong negative bay in the *Dst* index, of about -300 nT (see Fig. 2, top). The airglow history around this event is well documented in our data at

El Leoncito, during all the nights from July 12 to 18. The corresponding variations of OH temperature, OH band intensity, O₂ temperature, and O₂ band intensity are also shown in Fig. 2, together with the mean values for each night (horizontal dashed lines). Because of the lunar background correction that we use (Scheer and Reisin, 2001), our data are completely reliable, except when the moon passed closest to zenith (causing gaps in the figure).

The Bastille event occurs only 20 minutes before the end of the night at El Leoncito, when a prompt atmospheric influence from the sunlit side is unlikely. A possible reaction in our airglow data cannot be expected before the following night (July 14/15). Nocturnal means for all airglow parameters show indeed an enhancement in comparison to all the neighbouring nights in Fig. 2, and this enhancement gradually dies down in the following nights. The airglow anomaly for OH intensity has caught our attention before, but its eventual link to the Bastille event was not followed up (Scheer et al., 2005b). As the figure shows, the very high OH intensity at the beginning of the night is even more distinctive than the elevated nocturnal mean. Such a behaviour is absent in the other parameters.

On the other hand, during and after the geomagnetic storm on July 15/16, none of the four airglow parameters show any unusual behaviour in their nocturnal means. There is also no conspicuous airglow response to this storm in the nocturnal variations in the same, and the following nights, which only exhibit a slow modulation, probably of tidal origin (see Fig. 2).

3.3. *Are there airglow effects for the strongest X-ray flares?*

At this step, we present a systematic search for airglow signatures corresponding to solar X-ray flares. Table 2 gives the ranking of the main X class flares between August 1997 and February 2003. According to the timing of each flare, we inspected the temporal variation of the airglow data following the event.

For 18 of the 36 X-ray events shown, we have airglow data available. Only 3 or 4 of these are accompanied by airglow signatures that are potential candidates for a solar response. One case (#5 in the ranking) is the Bastille event already discussed. The others are three consecutive flares at 8:24 and 22:19 UT on 18 August 1998 and at 21:45 on the next day (with ranks #19, #8, and #11, resp.). The 8:24 UT event occurs 3 hours before the end of the nocturnal data acquisition, and coincides with the start of an increase of O₂ intensity, but this is probably too early for a causal relationship because of the time necessary for the solar disturbance to travel into the night sector. The flares #8 and #11 occur 50 and 90 minutes, respectively, before the beginning of the airglow observations, when the mesopause region over El Leoncito was still sunlit. Therefore, the chance of affecting airglow at the start of the night was much better. The airglow signals are moderately enhanced during the first few night hours in OH intensity (and also the other parameters, for flare #8), so that in these cases there is the possibility of a relation to the flares.

On the other hand, 14 flares are not accompanied by any noticeable airglow response. This includes especially the very strong X14 flare of 15 April 2001 (rank #2), and also the most prominent F10.7 anomaly (96 solar flux units above the level of the neighbouring days) of 12 July 2000 (#33), both mentioned before. However, most of these flares occur at local night, which reduces the chance of a detectable airglow effect, as mentioned. Only 5 cases correspond to local daytime (#2, #17, #22, #25, and #28) which converts them into possible counter-examples (against a solar link). Because of the timing of these flares, the absence of an airglow effect might be a consequence of the decay of the supposed atmospheric disturbance before night falls, if we assume that its lifetime is short, as was observed in far UV dayglow (see Tsurutani et al., 2005). Flare #17 occurs 3h 40min before the beginning of the night, while the other 4 cases happen before local noon. If the atmospheric disturbance lasts less than a few hours, then there would not have been a chance of an airglow effect, in any of these cases. All this suggests that the only two cases to expect an airglow response if the atmospheric disturbance is indeed short-lived, are the cases #8 and #11 on 18 and 19 August 1998 when effects were actually observed.

There is no use in attempting a systematic search for airglow signatures corresponding to the principal events identified by the other solar proxies, because as mentioned before, F10.7 data are only sampled once each day, and because of the limitation in using daily averages of EUV data. We have only done a visual inspection of a number of airglow nights corresponding to the major solar events in these proxies, without finding any significant example of a probable correlation.

3.4. *Are there airglow effects for the strongest geomagnetic storms?*

The geomagnetic storm of 15/16 July 2000 (following the Bastille event), which showed no airglow response as mentioned, was the strongest of all the storms for which we have airglow data. The ranking table analysis reveals that there are another 40 cases with storms of at least -100 nT and simultaneous (or followed by) airglow data. With only 3 exceptions, none of these events have conspicuous airglow effects that would be distinguishable from intrinsic nocturnal and day-to-day variability. This negative result is most relevant for the 6 strongest cases with $Dst < -200$ nT, because for the weaker storms it is reasonable to expect also a weaker atmospheric response. Neither are the 3 exceptions very plausible candidates for storm effects, for the following reasons. The first case, a massive but relatively slow OH intensity drop (over about 1 hour) on 24 May 2000, occurs 17 hours after the maximum Dst excursion of -147 nT. A very fast (12 minutes) drop in OH intensity on 29 October 2000 practically coincides with the storm maximum (-127 nT), and may be a mesospheric bore event similar to (but weaker than) the events we observed in August 2001 described in [Smith et al. \(2006\)](#). The third case (-109 nT) corresponds to strong surges in nocturnal mean OH and O₂ intensities on 23 and 24 May 2002, which were associated with horizontal wind perturbations at a remote site ([Scheer et al., 2005b](#)). The three cases are morphologically very different, with a wide range of time scales, and while their causes are unknown, a relation to geomagnetic storms would be unexpected, especially in view of the relatively small storm strengths involved.

Practically all this evidence points toward the absence of a noticeable influence of geomagnetic storms on mesopause region airglow and temperatures, at lower midlatitudes. This is consistent with the conclusions by [Fagundes et al. \(1996\)](#) for 23°S, who found no significant change in the nocturnal means of OH and O₂ temperatures that could be related to the geomagnetic storm of 9 July 1991.

3.5. *Are there solar causes for the strongest airglow events?*

One way to define airglow events is in terms of the anomaly of nocturnal means with respect to the neighbouring nights (which we briefly call “burst”), as was done in our paper just mentioned ([Scheer et al., 2005b](#)). However, this method did not produce more hits than drawing attention to the Bastille event. As an alternative, one could also point to the characteristic temporal variation observed in OH intensity (see Fig. 2) and search for cases with high airglow intensity at the beginning of the night, which might be signatures of solar flares occurring previously during daytime. As a simple criterion for such a search, we look for nights when the average intensity during the first 20 minutes divided by the long-term mean (I_{20}) is at least 2. Of course, this is not limited to an initial intensity decay, but also includes cases with high intensity during most of the night that qualify as bursts.

The ranking obtained for OH intensity is a list of 49 nights, with a maximum I_{20} of 3.03. A detailed inspection of the main 25 cases ($I_{20} \geq 2.14$) reveals that 9 exhibit the characteristic initial intensity drop (with 14/15 July 2000 appearing in the second place), 11 cases have high intensity throughout the night (including bursts), 3 show a slow decline, and 2 nights have insufficient data. None of these show any exceptional solar or geomagnetic activity, in any of the four proxies, with the Bastille event being the only exception. For 3 cases in 2006 for which the proxy information is incomplete, the absence of solar events can also be ascertained (C. H. Mandrini, personal communication).

The same analysis for O₂ intensity (a list of only 14 nights, $2.00 \geq I_{20} \geq 2.73$) detects 4 nights with initial intensity drop and 6 high intensity nights, while in the remaining 4 cases, the data start too late for a clear classification. The only tentative candidate case of a solar relationship may be 16/17 May 2000 (with $I_{20} = 2.21$), which follows a weak F10.7 anomaly (by 28 sfu), but without evidence in the other proxies.

To illustrate the nocturnal variations of some of the main cases, Fig. 3 shows the variation of OH intensity for three typical examples (the other 6 cases look similar): the night following the Bastille event (repeated here as a reference; $I_{20} = 2.95$), together with 11/12 June 1999 ($I_{20} = 2.67$) and 23/24 April 2006 ($I_{20} = 3.03$). It is clear from the figure that the shape of the initial part of the Bastille case is by no means unique in comparison with the two other examples corresponding to quiet solar and geomagnetic conditions. Thus, the hypothesis that the Bastille flare was the cause of the airglow behaviour on 14/15 July 2000 is severely weakened. This does not exclude the possibility of a minor airglow effect hidden under the dominant signature.

3.6. Intrinsic atmospheric dynamics

Since we discard a solar link for the conspicuous nocturnal airglow variations of the type present after the Bastille flare (and shown in Fig. 3), it is appropriate to look for an alternative explanation of these exceptional cases that represent not more than 1% of all the nights of observation.

Spectral analysis shows that the nocturnal variations can be essentially explained as a superposition of 2 principal oscillations in the tidal period range (3 to 24 hours), and eventually trends. By employing our method of iterative least-squares fitting (e.g., see [Reisin and Scheer, 2001](#)), spectral parameters can be determined with good precision, without problems with unequal data spacing (or even gaps). For the night of 14/15 July 2000, we find that the OH intensity variation is due to oscillations with periods of 4.6 and 6.6 h. This is close to the period of the main temperature oscillation of 5.2 h. By using the [Hines and Tarasick \(1987\)](#) theory, we can relate the amplitudes and phases of these oscillations to the vertical propagation of gravity waves or tides (as discussed by [Reisin and Scheer, 1996](#)).

The results are given in Table 3. There are two possible ways to relate the intensity and temperature oscillations. By using the closest period match, we find Krassovsky's ratio of the relative intensity and temperature amplitudes, $\eta = 6.8$, a phase shift between both oscillations, $\phi = -20^\circ$, and consequently a vertical wavelength $\lambda_z = -54$ km (the negative sign meaning downward phase propagation, and therefore upward energy propagation). The other possibility (using the 6.6 h intensity oscillation) also leads to an upward propagating wave with a not very different value of η but a shorter wavelength (28 km). This alternative is however less plausible because of the large value of ϕ beyond the theoretical limit of -90° . At any rate, this indicates that the observed nocturnal variation may be nothing but a superposition of upward-propagating gravity waves with amplitudes and vertical wavelengths in the normal range.

The same analysis was applied to the night of 23/24 April 2006 (see Table 3). Besides a trend component, there is an approximately terdiurnal oscillation in OH intensity and temperature. This again corresponds to an upward-propagating gravity (or tidal) wave with 44 km vertical wavelength. The principal spectral component for the O₂ emission is a strong semidiurnal wave (in both parameters), which surprisingly has nearly the same Krassovsky ratio and phase shift as the terdiurnal OH wave. The temperature amplitude of 15 K is not unusual for a semidiurnal tide ([Reisin and Scheer, 1996](#)), which thus appears to be a reasonable interpretation.

We may therefore conclude that the unusual shape of these nocturnal variations is just due to a chance combination of the timing and superposition of otherwise normal tidal and gravity waves. The values of η mean that relative intensity amplitudes cause more noticeable nocturnal variations than temperatures. That a greater number of cases occur in the OH rather than the O₂ emission is probably just a consequence of the typical tidal advance of the phase at this upper airglow layer.

4. Conclusions

Among more than 1400 nights of observations of mesopause region airglow in the OH(6-2) and O₂b(0-1) bands and the corresponding rotational temperatures, we find only weak evidence of solar events affecting brightness or temperature. Although there is a conspicuous OH intensity signature following the strong "Bastille Day" solar flare, a similar feature was also present in several nights under solar and geomagnetically quiet conditions, and therefore does not point to a solar link. However, there is maybe a

solar link for the enhanced airglow signals at the beginning of the nights 18/19 and 19/20 August 1998, shortly after strong X-ray flares. The absence of airglow signatures in many other cases with less favourable timing suggests that airglow effects do not last more than a few hours. Such a prompt response, if confirmed, would be surprising in view of the slow reaction of atomic oxygen advection under normal conditions. It would be understandable if the solar flare affected the mesopause region via a dynamical perturbation excited at higher altitude.

There was not a clearly discernible reaction in our airglow data to geomagnetic storms, even those as strong as about 300 nT. If long-lived effects of solar and geomagnetic disturbances exist at all, they do not separate clearly from normal intrinsic atmospheric behaviour, so that their detection would require more data than available.

When starting from the most prominent features in the nocturnal variation of airglow brightness, we find no signs of corresponding solar or geomagnetic signatures. These features are probably mainly due to intrinsic dynamics (tides and gravity waves). Such events are quite rare (appearing in no more than a few percent of the nights), although the corresponding wave parameters are not unusual.

A possible reason why we have not found more (strong) airglow signatures may simply have to do with observational conditions and the short lifetime of the atmospheric disturbance. On the one hand, solar events that occur during local night at the airglow observation site can be expected to affect nocturnal observations only if horizontal transport between the sunlit and dark hemispheres is fast enough. On the other hand, if the solar event occurs during the local day at the observing site, its effects could have died down before the immediately following night (if our conclusion about the short lifetime of the mesopause airglow response is correct). Then, daytime observations would have a much better chance of detecting those events in the atmosphere.

Acknowledgements

We are grateful for helpful discussions with our colleagues Cristina H. Mandrini and María Luisa Luoni. We also thank the colleagues and their institutions who make the solar and geomagnetic data available on the internet. Funding through ANPCyT PICT 12187 and CONICET PIP 6269/2005 is acknowledged.

References

- Balan, N., Kawamura, S., Nakamura, T., et al. Simultaneous mesosphere/lower thermosphere and thermospheric F region observations during geomagnetic storms. *J. Geophys. Res.* 109(A4), A04308, doi:10.1029/2003JA009982, 2004.
- Beig, G., Keckhut, P., Lowe, R.P., et al. Review of mesospheric temperature trends. *Rev. Geophys.* 41(4), 1015, doi:10.1029/2002RG000121, 2003.
- Brekke, P., Rottman, G.J., Fontenla, J., Judge, P.G. The ultraviolet spectrum of a 3B class flare observed with SOLSTICE. *Astrophys. J.* 468, 418-432, 1996.
- Fagundes, P.R., Sahai, Y., Takahashi, H., et al. Thermospheric and mesospheric temperatures during geomagnetic storms at 23° S. *J. Atmos. Terr. Phys.* 58(16), 1963-1972, 1996.
- Gonzalez, W.D., Tsurutani, B.T., Clúa de Gonzalez, A.L. Interplanetary origin of geomagnetic storms. *Space Sci. Rev.* 88, 529-562, 1999.
- Hines, C.O., Tarasick, D.W. On the detection and utilization of gravity waves in airglow studies. *Planet. Space Sci.* 35/7, 851-866, 1987.
- Jackman, C.H., DeLand, M.T., Labow, G.J. The influence of the several very large solar proton events in years 2000-2003 on the neutral middle atmosphere. *Adv. Space Res.* 35(4), 445-450, 2004.

- Mannucci, A.J., Tsurutani, B.T., Iijima, B.A., et al. Dayside global ionospheric response to the major interplanetary events of October 29-30, 2003 "Halloween Storms". *Geophys. Res. Lett.* 32, doi:10.1029/2004GL021467, L12S02, 2005.
- Meier, R.R., Warren, H.P., Nicholas, A.C., et al. Ionospheric and dayglow responses to the radiative phase of the Bastille Day flare. *Geophys. Res. Lett.* 29(10), doi:10.1029/2001GL013956, 2002.
- Reisin, E.R., Scheer, J. Characteristics of atmospheric waves in the tidal period range derived from zenith observations of O₂(0-1) Atmospheric and OH(6-2) airglow at lower midlatitudes. *J. Geophys. Res.* 101, 21223-21232, 1996.
- Reisin, E.R., Scheer, J. Vertical propagation of gravity waves determined from zenith observations of airglow. *Adv. Space Res.* 27(10), 1743-1748, 2001.
- Scheer, J. Programmable tilting filter spectrometer for studying gravity waves in the upper atmosphere. *Appl. Opt.* 26, 3077-3082, 1987.
- Scheer, J., Reisin, E.R. Refinements of a classical technique of airglow spectroscopy. *Adv. Space Res.* 27(6-7), 1153-1158, 2001.
- Scheer, J., Reisin, E.R., Mandrini, C.H. Solar activity signatures in mesopause region temperatures and atomic oxygen related airglow brightness at El Leoncito, Argentina. *J. Atmos. Solar-Terr. Phys.* 67(1-2), 145-154, 2005a.
- Scheer, J., Reisin, E.R., Batista, P.P., et al. Detection of meteor radar wind signatures related to strong short-duration day-to-day airglow transitions at sites 2600 km apart. *J. Atmos. Solar-Terr. Phys.* 67(6), 611-621, 2005b.
- Smith, A.K., Marsh, D.R. Processes that account for the ozone maximum at the mesopause. *J. Geophys. Res.* 110(D23), D23305, doi:10.1029/2005JD006298, 2005.
- Smith, S.M., Scheer, J., Reisin, E.R., et al. Characterization of exceptionally strong mesospheric wave events using all-sky and zenith airglow observations. *J. Geophys. Res.* 111(A9), A09309, doi:10.1029/2005JA011197, 2006.
- Tsurutani, B.T., Judge, D.L., Guarnieri, F.L., et al. The October 28, 2003 extreme EUV solar flare and resultant extreme ionospheric effects: Comparison to other Halloween events and the Bastille Day event. *Geophys. Res. Lett.* 32(3), L03S09, doi:10.1029/2004GL021475, 2005.

Table 1

Number of nights with airglow data from El Leoncito (31.8°S, 69.3°W), Buenos Aires (34.6°S, 58.4°W; in 1994), and El Arenosillo (Spain) (37.1°N, 6.7°W; in 1990):

	jan	feb	mar	apr	may	jun	jul	aug	sep	oct	nov	dec	total
1986						5	14			6	10		35
1987									17				17
1990	13	26	10										49
1992										16			16
1994										2	22	6	30
1997								23	21	6	13	9	72
1998	8	1		23	17	26	18	25	9	25	26	14	192
1999	15	12	17	20	9	29	28	11	12	17	21	10	201
2000	15	17	20	20	25	15	14	23	18	26	16	17	226
2001	22	20	16	23	23	11		24	14	24	10	10	197
2002	22	10	22	19	15	27	29	31	30	28	18	29	280
2003	12												12
2006		22	27	30	31	24							134
sum:	108	108	112	135	120	137	103	137	121	150	136	95	1461

Table 2

Ranking of strongest X-ray flares (Aug 1997-Feb 2003) and possible airglow response. Date and time of the maximum are given in Universal Time. Flare class is in units of 10^{-4} W/m² for X class events, for emissions in the spectral range 0.1 to 0.8 nm. A match with an EUV or F10.7 proxy event is marked by a star. For completeness, also events for which we have no airglow observations are included (no entry in “airglow effect” column).

#	UT date	peak	Class	EUV	F107	airglow effect?
01	02APR01	21:51	X20			
02	15APR01	13:50	X14	*		no response
03	06NOV97	11:55	X9.4			
04	13DEC01	14:30	X6.2			
05	14JUL00	10:24	X5.7	*		BASTILLE, strong initial IOH
06	25AUG01	16:45	X5.3			
07	06APR01	19:21	X5.0			
08	18AUG98	22:19	X4.9			high initial intensities, temperatures
09	23JUL02	00:35	X4.8			
10	26NOV00	16:48	X4.0	*		
11	19AUG98	21:45	X3.9			high initial IOH
12	22NOV98	06:42	X3.7			
13	28DEC01	20:45	X3.4	*		
14	20JUL02	21:30	X3.3			
15	28NOV98	05:52	X3.3			no response
16	24AUG02	01:12	X3.1	*		
17	15JUL02	20:08	X3.0			no response
18	11DEC01	08:08	X2.8			
19	18AUG98	08:24	X2.8			simultaneous IO2 increase
20	06MAY98	08:09	X2.7			
21	24SEP01	10:38	X2.6	*		no response
22	27NOV97	13:17	X2.6			no response
23	22NOV98	16:23	X2.5			
24	10APR01	05:26	X2.3			no response
25	06JUN00	15:25	X2.3			no response
26	24NOV00	15:13	X2.3			
27	23NOV98	06:44	X2.2			no response
28	20MAY02	15:27	X2.1			no response
29	04NOV97	05:58	X2.1	*		
30	12APR01	10:28	X2.0			no response
31	24NOV00	05:02	X2.0			
32	25NOV00	18:44	X1.9	*		
33	12JUL00	10:37	X1.9	*		no response
34	18JUL02	07:44	X1.8			no response
35	24MAR00	07:52	X1.8			no response
36	14OCT99	09:00	X1.8	*		no response

Table 3

Main spectral components and wave parameters for two nights of special airglow variations (see text for details).

date	airglow layer	Intensity period[h]	Temperat. period[h]	Intensity rel. ampl.	Temp. ampl. [K]	η	ϕ [°]	λ_z [km]
14jul00	OH	4.63	5.18	19%	5.2	6.8	-20	-54
	OH	6.55	"	14%	"	5.0	-116	-28
23apr06	OH	7.57	7.60	25%	6.8	6.7	-24	-44
	O ₂	12.95	11.86	51%	15.3	6.8	-25	-48

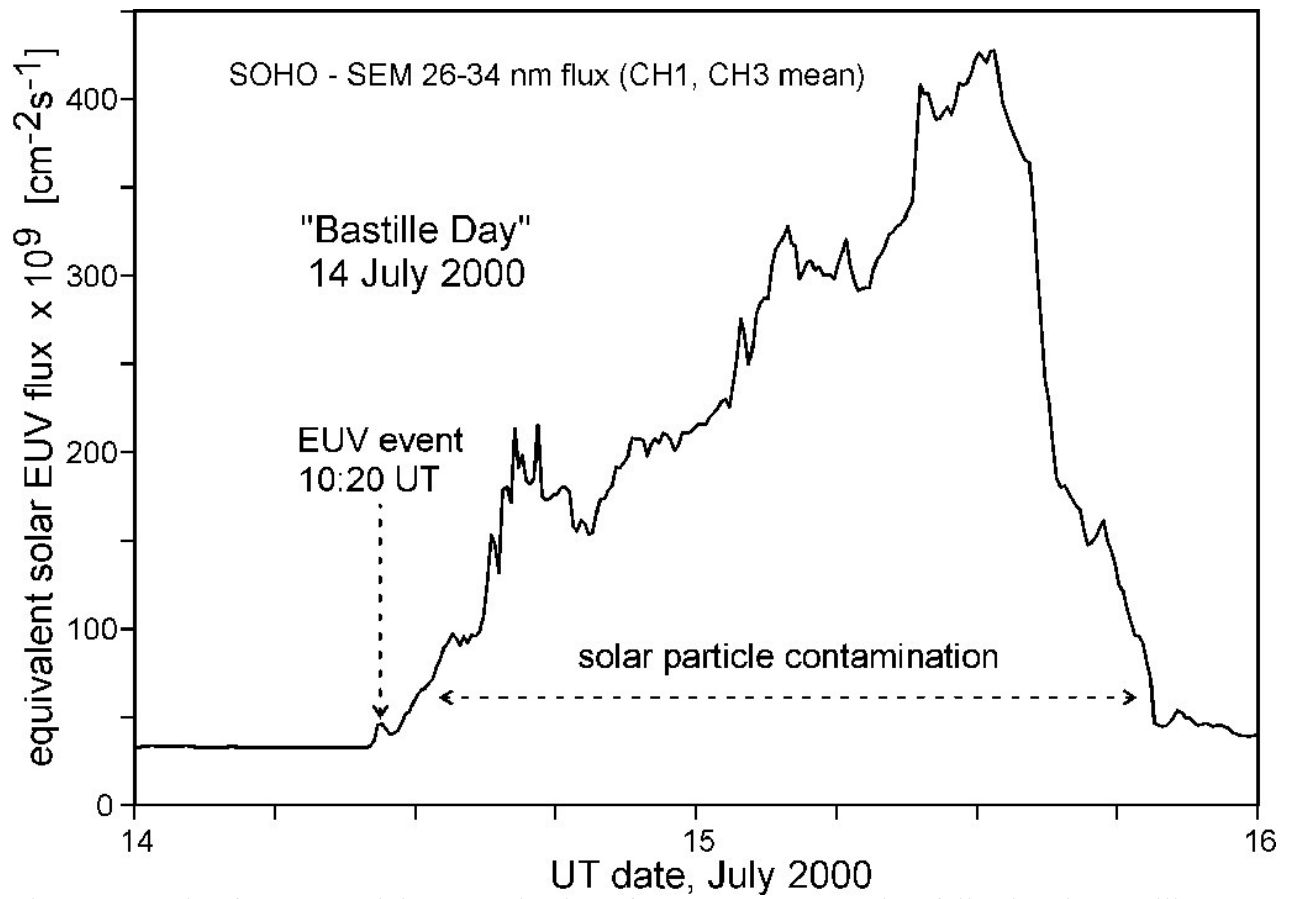


Fig. 1. Example of strong particle contamination of SOHO-SEM EUV data following the Bastille Day flare.

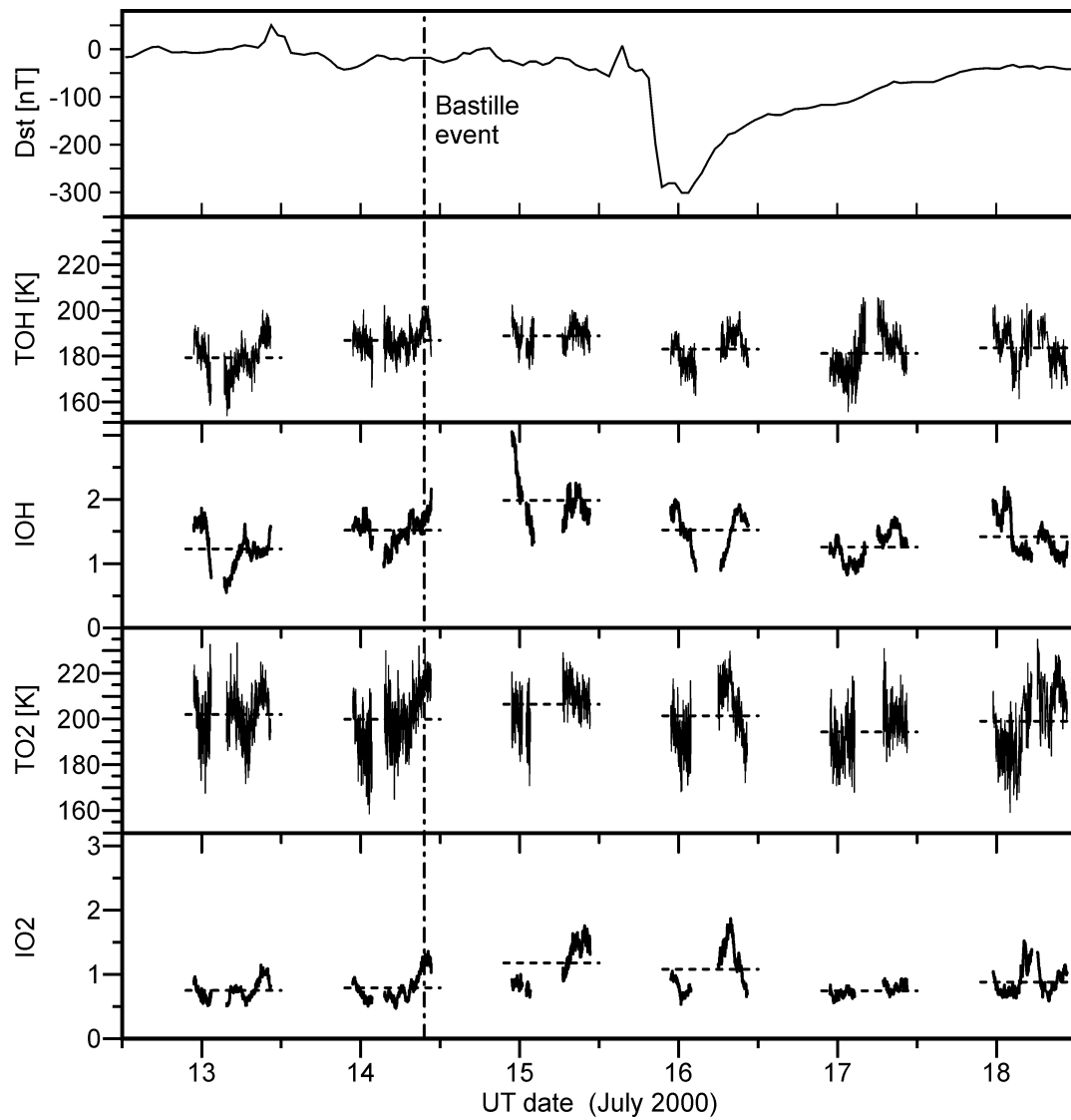


Fig. 2. Temporal variation of (from top to bottom panel): *Dst* index, OH rotational temperature, OH band intensity, O₂ rotational temperature, and O₂ band intensity around the Bastille Day flare of 14 July 2000 (vertical dash-dotted line). Horizontal dashed lines mark nocturnal airglow means.

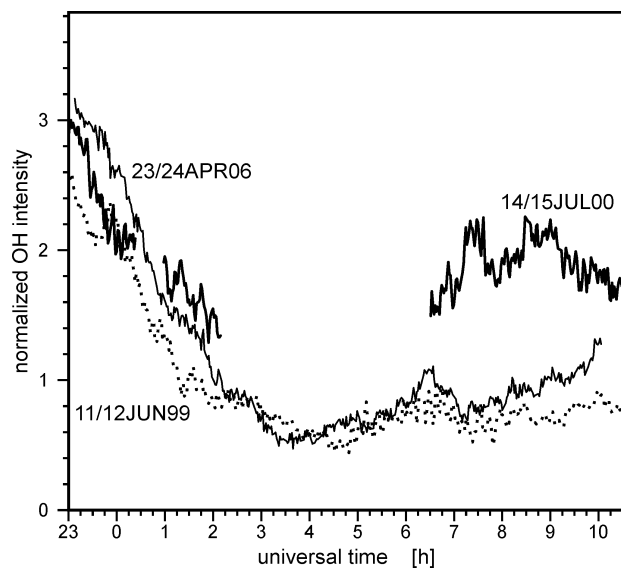


Fig. 3. Nocturnal variation of OH intensity during the nights of 11/12 June 1999 (dotted line), 14/15 July 2000 (fat solid lines, separated by 2 data gaps), and 23/24 April 2006 (thin solid line).